Article

Land use and cover change accelerated China's land carbon sinks limits soil carbon

Check for updates

Yue Cheng[1,2], Peng Luo[1,2]✉, Hao Yang[1], Mingwang Li[3], Ming Ni[1,2], Honglin Li[1,2], Yu Huang[1,2], Wenwen Xie[1,2] & Lihuan Wang[2,4]

Land use and cover change (LUCC) significantly impacts global carbon cycles and land surface properties, accounting for 25% of the historical atmospheric CO_2 increase. We explore a previously overlooked role of LUCC in driving the land carbon cycle by using a three-level meta-analysis and Land Use Harmonization data to drive an ecosystem model. Our findings reveal that a loss of 39.2% of soil organic carbon (SOC) change in China due to LUCC, mitigated by afforestation, doubles gross primary productivity at 0.02 Pg C yr^{-1}, countering central China's urbanization decline. Indirect climate effects, especially soil bulk density, significantly impact SOC compared to direct climate effects. LUCC has significantly increased the Chinese terrestrial carbon sink, with net ecosystem productivity reaching 0.02 ± 0.12 Pg C yr^{-1}. Our study underscores the importance of reforestation and afforestation in addressing climate change and enhancing carbon sinks in future carbon management.

Contemporary terrestrial ecosystems undergo extensive transformation due to human land use and management practices[1]. Anthropogenic land use and cover change (LUCC) have significantly altered global element cycles, water cycles, and the land surface at various scales[2–4]. LUCC plays a pivotal role in shaping Earth's ecological environment and the carbon cycle of terrestrial ecosystems by altering land-atmosphere interactions and surface attributes[5]. LUCC-induced carbon emissions, accounting for 25% of the historical atmospheric CO_2 increase, were estimated with large uncertainty at 1.3 ± 0.7 Pg C yr^{-1} for the last decade[6], complicating the global Carbon budget[7–9].

Soil organic carbon (SOC) is vital for soil health, food production, water supply regulation, and climate change mitigation[10,11]. With a carbon storage capacity exceeding that of vegetation biomass and atmospheric carbon stocks, SOC provides significant benefits to both human societies and the environment[12,13]. LUCC driven by population growth, has significantly impacted SOC dynamics, leading to a decline in storage due to intensive land management[14]. Furthermore, the land carbon cycle can be dissected into two distinct components: LUCC-C-cycle, representing the carbon balance over lands under direct human land use, and NO-LUCC, which characterizes carbon dynamics over lands unaffected by direct human alterations, influenced instead by global environmental changes such as atmospheric CO_2 concentration, climatic variations, and nitrogen deposition[1].

Currently, methodologies for assessing the impacts of LUCC on the carbon cycle at regional and global scales primarily employ a combination of approaches. These include list methods such as the Tier 1 method outlined by the Intergovernmental Panel on Climate Change (IPCC), which are simplified approaches for estimating greenhouse gas emissions or removals that require minimal data and resources. Additionally, modeling techniques utilizing remote sensing and process-based ecosystem models are utilized in this assessment[15,16]. Dynamic Global Vegetation Models (DGVMs) are integral components of the Global Carbon Budget (GCB8), facilitating simulations of carbon uptake and release processes, focusing on various drivers such as rising atmospheric CO_2, climate change, nutrient deposition, land use, land use change, and carbon sinks[17]. The Land-Use Harmonization (LUH2) dataset serves as a foundation for carbon modeling, drawing from country-level agricultural reports provided by the Food and Agriculture Organization (FAO) and integrating the History Database of the Global Environment (HYDE) land use model[17,18]. Models accurately simulate terrestrial carbon uptake but are uncertain due to initial input parameters, model error, and forecast differences[19]. This leads to significant differences in the effect of LUCC on land carbon among different models[20,21]. Meta-analyses have proven effective in statistically assessing the impact of LUCC on SOC[22–24]. To address inherent uncertainties and discrepancies among different models, a combined approach integrating

[1]CAS Key Laboratory of Mountain Ecological Restoration and Bioresource Utilization & Ecological Restoration and Biodiversity Conservation Key Laboratory of Sichuan Province, Chengdu Institute of Biology, Chinese Academy of Sciences, Chengdu, China. [2]University of Chinese Academy of Sciences, Beijing, China. [3]Qinghai University, Xining, China. [4]Institute of Mountain Hazards & Environment, Chinese Academy of Sciences, Chengdu, China. ✉e-mail: luopeng@cib.ac.cn

meta-analysis and modeling offers a comprehensive framework for evaluating the effects of LUCC on the land carbon cycle.

China has undergone large-scale LUCC, including deforestation, cropland expansion, and afforestation since 1900[17]. Initiatives such as the "Grain for Green" project, initiated in 1999, have aimed to convert cropland into forest, shrubland, or grassland to mitigate the impacts of population growth and increasing demands for agricultural resources[22,24]. National policies such as the Three-North Shelterbelt Forest, Natural Forest Conservation Program, and Grain For Green Project (GFGP) have led to significant land use and cover transformations, particularly in the Loess Plateau[23]. However, the precise impact of LUCC on China's carbon budget remains to be determined, primarily due to methodological inconsistencies, the absence of comprehensive long-term LUCC databases, oversimplified models depicting forest carbon dynamics, and inadequate consideration of various forest types or management practices[17]. Addressing these limitations is crucial to understanding the relationship between LUCC and carbon dynamics in China[1,23,25].

Here, we used a combination of meta-analysis and process-based Earth system modeling using the U.S. National Center for Atmospheric Research's Community Earth System Model version 2 and the data-driven machine learning approach to generate a comprehensive estimate of the impacts of LUCC on land carbon dynamics in China. Initially, we conducted a thorough analysis using previous observations, employing a three-level meta-analysis and a data-driven machine learning approach to assess the effects of LUCC on changes in SOC and to identify key influencing factors in China. Subsequently, we used the LUH2 dataset to drive a process-based land ecosystem model, deriving the resultant carbon cycle. These simulations were then compared with flux data collected from nine ChinaFlux sites. Our objective was to evaluate the impacts of LUCC on carbon storage dynamics and carbon fluxes in Chinese terrestrial ecosystems from 1979 to 2014. This is particularly relevant given the intensive expansion of forests observed since 1980[17]. Conversely, the LUCC-free scenario (no LUCC) primarily considered the impacts of climate, nitrogen deposition, and CO_2 fertilization on the carbon cycle.

Methods
Meta-analysis of previous studies on the SOC in China
We conducted a comprehensive three-level meta-analysis to examine the impact of LUCC on SOC dynamics across various land-use types in China. Our analysis synthesized the findings of 132 publications (1248 observations) paired meta-analyses on SOC (Supplementary Fig. 1, Supplementary Fig. 2) on different climate zones and regional types (Supplementary Fig. 3). We first performed a systematic search for peer-reviewed meta-analyses on SOC stocks or concentrations using various databases, including the Web of Science (Core Collection; http://www.webofknowledge.com), Scopus, the China National Knowledge Infrastructure (CNKI; https://www.cnki.net) and the Google Scholar (http://scholar.google.com). The search was done on November 9th, 2023, and updated on January 1st, 2024, using the following search string: ("meta*analysis" OR "systematic review") AND ("land use change" OR "land cover") AND ("soil organic carbon" OR "SOC" OR "soil organic matter" OR "SOM" OR "soil carbon") in title, abstract, and keywords fields. We screened the titles and abstracts of the 3125 identified papers for their potential inclusion in our study. A paper had to (i) analyze the effect of one or several factors on bulk SOC stocks or concentrations, (ii) the same stratified method for soil sampling must have been employed for reference plots, and samples must be collected to a depth of at least 10 cm, (iii) present indicators of precision of the effect sizes (standard errors or confidence intervals). Finally, a total of 132 studies were retained. A list of the publications considered in this systematic review with meta-analysis is given in Supplementary Data. The literature review was conducted following the Preferred Reporting Items for Systematic Reviews and Meta-Analyses (PRISMA) guidelines[26]. A PRISMA flow diagram depicting the literature selection procedure is provided in Supplementary Fig. 2. When different publications included the same data, we recorded the data only once. Some studies exclusively reported soil organic matter (SOM). Soil organic carbon concentration (SOC) (g/kg) values were calculated as follows[27]:

$$SOC = SOM \times 0.58 \qquad (1)$$

All effect sizes extracted from the 132 meta-analyses included in our study were meticulously digitized from textual descriptions, tables, or figures using the Plot Digitizer software (http://plotdigitizer.sourceforge.net/) and systematically recorded in an Excel spreadsheet. Following IPCC standards, we carefully documented the corresponding land-use types for each effect size. Additionally, we collected relevant metrics such as ratios, percentage changes, potential transformations (e.g., logarithm), confidence intervals, and other variability indicators, along with the number of primary studies and observations used for effect size calculations. By compiling lists of primary studies for each meta-analysis, we were able to identify common primary studies among different pairs of meta-analyses. Finally, we assessed the meta-analyses included in our study against eight quality criteria related to the literature search, statistical analyses, and potential bias analysis. It is crucial to note that a flawed methodology in retrieving primary studies and analyzing data can lead to biased and misleading results.

In estimating the impact of LUCC on SOC in China, we explored several meta-analytical models, varying in the structure of their random effects, the inclusion or exclusion of the quality score of the first-order meta-analyses, and the redundancy of primary studies between meta-analyses. The optimal model for each factor was selected based on the Akaike information criterion (AIC)[28]. The most intricate model is a three-level meta-analytical model, incorporating a variance-covariance matrix considering the precision, quality, and redundancy of the first-order meta-analyses. This model is formulated as follows:

$$\begin{aligned} \text{Level 1 model}: Y_{ij} &= \lambda_{ij} + e_{ij} \\ \text{Level 2 model}: \lambda_{ij} &= \kappa_j + \mu_{(2)ij} \\ \text{Level 3 model}: \kappa_j &= \beta_0 + \mu_{(3)j} \end{aligned} \qquad (2)$$

The three-level random effects model uses three sources of variances: sampling variance of observed effect sizes, variance within the same study, and variance between studies. The Y_{ij} represents the ith effect size in the jth study, λ_{ij} represents the true effect size, $Var(e_{ij})$ represents the known sampling variance, κ_j represents the average effect, β_0 represents the average population effect, and Var and Var are the study-specific level 2 and level 3 variances.

We used the inverse variance to weight each effect size, following recommendations by Marín-Martínez and Sánchez-Meca[29]. We also adjusted the weight of lower-quality meta-analyses based on criteria from Doi et al.[30]. Quality assessment was conducted by evaluating the percentage of eight quality criteria met by each meta-analysis, with detailed criteria explanation available in ref.[31]. To address non-independence between effect sizes of different meta-analyses, we calculated a variance-covariance matrix based on pseudo correlation[32]. The proxy for correlation between each pair of meta-analyses was estimated as $(2 \times m)/(n1 + n2)$, where m represents the number of common primary studies, and $n1$ and $n2$ denote the total number of primary studies in each respective meta-analysis.

The maximum likelihood estimation method is used to compute parameter estimates, including the Q statistic and I^2 statistic. To address the "file-drawer problem," the presence of publication bias in meta-analyses was examined. A funnel plot was employed to assess the presence of bias, with a symmetric distribution indicating its absence. Publication analyses were conducted using the Tandem Procedure, and Rosenthal's "fail-safe N" method, Egger's regression test, and Begg's correlation test were applied to evaluate potential bias. The p values from these tests, all exceeding 0.05, indicate a lack of sufficient evidence to suggest publication bias. These analyses were performed using the *rma.mv* function of the metafor package within the R statistical software environment, facilitating the modeling of a three-level random-effects model.

Statistical analyses

We employed a combination of Random Forest modeling, simple linear regression, correlation analyses, and Structural Equation Modeling (SEM) to analyze our meta-analysis results. Specifically, we utilized Random Forest Models for visualizing patterns and determining variable importance. Simple Linear Regression and SEM were employed to assess the statistical significance and directionality of patterns. Additionally, correlation analyses were carried out to evaluate the linear relationships between pairs of variables.

First, we used Simple Linear Regression to explore the relationship between the Response Ratio of SOC (RR_{SOC}) and various environmental conditions. We specifically analyzed six environmental variables: (1) Mean Annual Temperature (MAT), (2) Mean Annual Precipitation (MAP), (3) elevation, (4) bulk density (BD), (5) soil background pH, and (6) duration.

Next, we included seven environmental predictors to derive a meta-forest model, a machine learning-based random forest model adapted for meta-analysis, to map the response of SOC stock/content to LUCC in China. These factors included climate conditions, soil properties (e.g., bulk density and initial soil pH), and conversion management (duration). Missing data were imputed using the *missForest* Package in R Studio. The importance of each variable was ranked using mean decrease accuracy (IncMSE%). Missing data were imputed using the *missForest* Package in R Studio, with the mean decrease accuracy (IncMSE%) utilized for ranking variable importance[3].

Then, we conducted correlation analyses to assess the associations between RR_{SOC} and each examined variable. Similar to previous studies[5,6], we also used SEM to investigate the direct and indirect impacts of climate, soil characteristics, and duration on RR_{SOC}. The modeling criteria for evaluating SEM fit, including comparative fit index, root mean square error of approximation, chi-square value (χ^2), and *p*-value were taken into account in this modeling[7]. SEM was conducted using the R package *lavaan* (version 4.3.2)[8].

Model overview

The Community Land Model. In order to demonstrate the effects of LUCC on plant productivity, carbon sink dynamics, and carbon storage in China, we utilized the CESM[33], which incorporates the Community Land Model (CLM) as its land component. Two experiments were carried out using CLM5, producing outcomes at a resolution of 0.25 × 0.25 for the time period from 1979 to 2014. The CESM, with its integrated CLM, allowed us to accurately simulate the biogeochemical and biogeophysical processes necessary for assessing the impacts of LUCC. The CLM5 model partitions the land surface into various categories including glacier, lake, wetland, urban, and vegetated land. Employing plant functional types (PFTs) instead of biomes, the model characterizes vegetation based on physiological and structural attributes, incorporating 16 PFTs such as bare ground, trees, crops, temperate/boreal shrubs, arctic/cool C_3 grasses, and warm C_4 grasses. These experiments, detailed in Supplementary Table 1, were undertaken with CLM5 to explore the influence of LUCC on the land carbon cycle[34]. We used the China Meteorological Forcing Dataset (CMFD) for meteorological data (Supplementary Table 2), while the LUCC data were sourced from the LUH2 dataset. The LUH2 dataset is derived from reports by the FAO which provide a breakdown of agricultural areas at the country level. This dataset integrates the HYDE and uses the model with the Miami-LU model in order to forecast the extent of forest coverage prior to human intervention[35]. Furthermore, it includes a simulation of secondary forest areas that are influenced by logging activities and expansion of agricultural land. A detailed overview of the method steps in CLM5 is provided in Supplementary Fig. 4.

Model validation. The CLM model was rigorously validated against observations to ensure a correct estimate of land carbon in this study. Specifically, simulated Gross Primary Productivity (GPP) was compared with data from nine carbon flux towers spanning the 2003–2010 period (Supplementary Table 3). The correlation between observed and estimated GPP is illustrated ($R^2 = 0.8$, $P < 0.001$, Supplementary Fig. 5), indicating a high degree of precision in the estimation.

Data processing. Initially, we calculated the yearly mean values of GPP, Net Ecosystem Productivity (NEP), and soil carbon stocks (at depths of 20 cm and 100 cm) across China, accounting for both scenarios with and without land-use change spanning from 1979 to 2014. Subsequently, we evaluated the escalation in carbon fluxes emanating from wood product pools to litter and fossil fuels, attributed to land use and land cover change. The Mann-Kendall method, a nonparametric test for monotonic trends, was employed to scrutinize trends in carbon cycle variables. This method, renowned for its resilience to outliers, has garnered favor for trend analysis. Trends in GPP and NEP were derived utilizing the entire 1979–2014 temporal dataset, with the robustness of trends corroborated through the non-parametric Mann-Kendall test and Sen's slope estimator.

Results

The overall effect of LUCC on SOC dynamics

The 1248 observations collected in our literature search included 132 publications across all major terrestrial ecosystems in China. The climate conditions sampled in these experiments span a broad range, from 38 mm to 3000 mm in mean annual precipitation and from −1.7 °C to 22.5 °C in mean annual temperature. Additionally, the experiments encompass altitudes ranging from 5 m to 4500 m, soil bulk densities from 0.62 g/m^{-3} to 1.66 g/m^{-3}, and soil pH values from 3.8 to 8.84 (Fig. 1). The majority of experiments were conducted in warm temperate ecosystems (52.41%), semi-acid areas (85.25%), and the Loess Plateau (54.55%) in China (Supplementary Fig. 3). The predominant land use type in these experiments is the conversion from crops to forests (38.14%) (Supplementary Fig. 3).

SOC changes had different responses to land use conversion in China. The overall effects of LUCC resulted in a loss of 39.2% of SOC change in China (Fig. 2). This study primarily focused on forest ecosystems, comprising the highest number of studies ($N = 549$, Supplementary Fig. 6). Changes in LUCC exert a negative effect on both SOC concentration and SOC stocks. Conversion of grassland to cropland (56%) is significantly higher SOC losses than forest to cropland (37%). The increased SOC was 11%, 13%, and 22%, respectively when the cropland was recovered to forest, grassland, and shrubland (Fig. 2). To verify these results and assess the potential influence of overlapping meta-analyses, we extracted all accessible unique effect sizes from the meta-analyses. The final data included 1248 unique effect sizes (Supplementary Fig. 7). Results of a random-effects meta-analysis corroborated results from the three-level meta-analysis (lnRR = −0.49, 95% CI [−0.32, 0.66], $P < 0.001$). Next, we tested the subgroup effects for (a) type of land use change type, (b) soc change, (c) climate zone, (d) humid and arid zone, (e) regional type, (f) elevation, (g) soil depth, (h) bulk density and (i) soil pH on SOC, as an approach to explaining the systematic variance (Supplementary Table 4). Conversions from forest-lands, grasslands, and other land categories to croplands consistently resulted in substantial SOC loss, with confidence intervals (CI) of [−2.53, −0.20], −1.16 (CI [−2.19, −1.30]), −1.74, and −3.1 (CI [−4.46, −1.73]), respectively (Fig. 3, Supplementary Table 5). Not surprisingly, the impact of LUCC was sensitive to climate in the following order from smallest to largest in terms of changes in SOC: Tropical (lnRR = −0.31, $P < 0.001$) < Temperate (lnRR = −0.54, $P < 0.01$) < Cold Plateau (lnRR = −0.72, $P < 0.001$). These results indicated that LUCC impacts on SOC change varied depending on climatic conditions influencing the plant and soil processes driving soil organic matter dynamics. Moreover, our analyses revealed a decrease in SOC change attributable to LUCC in arid regions of China, accounting for 21.33% of the total carbon loss in acidic regions. However, it is important to note that the specific impact of LUCC on SOC can vary significantly depending on the type of land use change and local conditions. Conversely, LUCC induced a significant positive effect on SOC change in the Loess Plateau (CI = 0.56, [−0.75, 1.44]). Notably, land-use changes negatively impacted SOC change across different elevations and soil
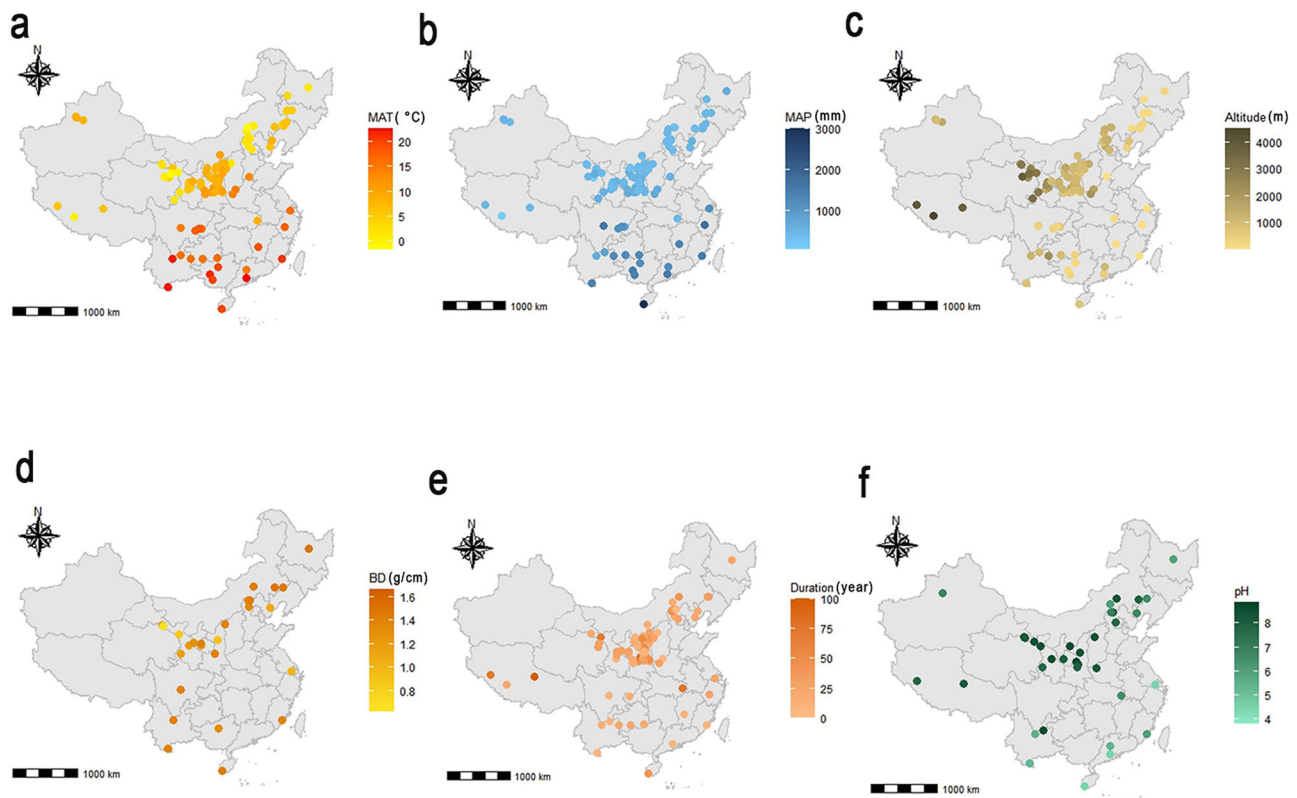
Fig. 1 | The distribution of 1248 meta-analysis plots with climate and other parameters in China. a Mean annual temperature (MAT), **b** Mean annual precipitation (MAP), **c** Altitude, **d** Bulk density (BD), **e** Duration, **f** Soil pH.
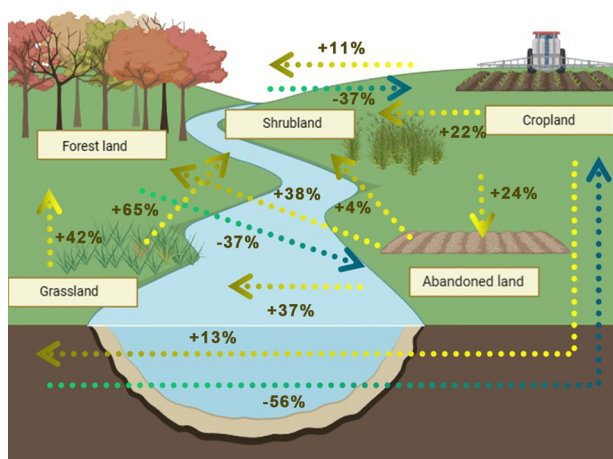

Fig. 2 | Conceptual model of SOC dynamics due to LUCC in the meta-analysis. The yellow arrow indicates an increase, while the blue arrow indicates a decrease.

depths, suggesting minimal influence from elevation and soil depth on LUCC-induced carbon dynamics. Additionally, the impact of land-use change on SOC change had a negative effect at bulk weights greater than 1.6 g/cm^{-3}. Besides, LUCC improves SOC in both acidic and neutral soils (lnRR = 0.38, $P < 0.01$ and 0.47, $P < 0.05$). However, it is important to note that the specific impact of LUCC on SOC can vary significantly depending on the type of land use change and local conditions (see the Discussion section).

Driving factors for soil carbon pool due to LUCC
We provided a detailed analysis of the distribution of these influencing factors across China (Fig. 1). MAP was correlated positively with SOC due to

LUCC ($n = 1162$, $R_{adj}^2 = 0.01$). In contrast, MAT showed a negative correlation with SOC due to LUCC ($n = 1162$, $R_{adj}^2 = -0.0008$), consistent with previous studies[36,37]. Lower SOC changes were observed at higher altitudes (Fig. 4). The impact of LUCC on SOC changes was particularly pronounced in acidic soils (Fig. 4). There was positive correlation between SOC and bulk density due to LUCC ($R^2 = 0.03$, $P < 0.001$). Changes in SOC were negatively affected by the timing of LUCC (Fig. 4).

LUCC activities like farming and deforestation accelerated SOC decomposition, influenced by factors like LUCC type and intensity. To evaluate the relative significance of climatic factors, soil characteristics, and other environmental variables, we employed a meta-forest, a random forest model adapted for meta-analysis, considering interactions among variables and potential nonlinearity (refer to the Methods section). Soil bulk density emerged as the most influential variable in explaining the variation in SOC due to LUCC (Fig. 5a). Following this, the duration became the second most critical factor controlling SOC dynamics, while MAP exhibited a comparatively lesser impact on the spatial pattern of SOC. These results suggest that soil properties played a crucial role in regulating SOC dynamics in response to land use changes. The RR of SOC was negatively correlated with the duration of LUCC. Pearson's correlation analysis revealed significant negative correlations among climate variables (MAP, MAT) and latitude ($p < 0.01$, Fig. 5b). Moreover, the RR of SOC was significantly positively correlated with MAP and BD but significantly negatively correlated with soil pH and duration. To delve deeper into the potential mechanisms of SOC RR concerning environmental and climatic factors, along with recovery time due to LUCC, SEM was employed (Fig. 5c). The results showed that indirect climate effects significantly impacted SOC compared to direct climate effects. Specifically, the SEM for SOC indicated that soil characteristics may have exerted direct and positive influences on SOC RR following LUCC (path coefficient = 0.08, Fig. 5c). Conversely, climatic factors appeared to indirectly influence SOC RR through environmental factors such as latitude and elevation (Fig. 5c).

Fig. 3 | Weighted effect sizes for soil organic carbon (SOC) changes under different land use changes. Error bars indicate the 95% confidence interval, with statistical significance denoted as follows: ***, $p < 0.001$; **, $p < 0.01$; *, $p < 0.05$; $p < 0.1$.
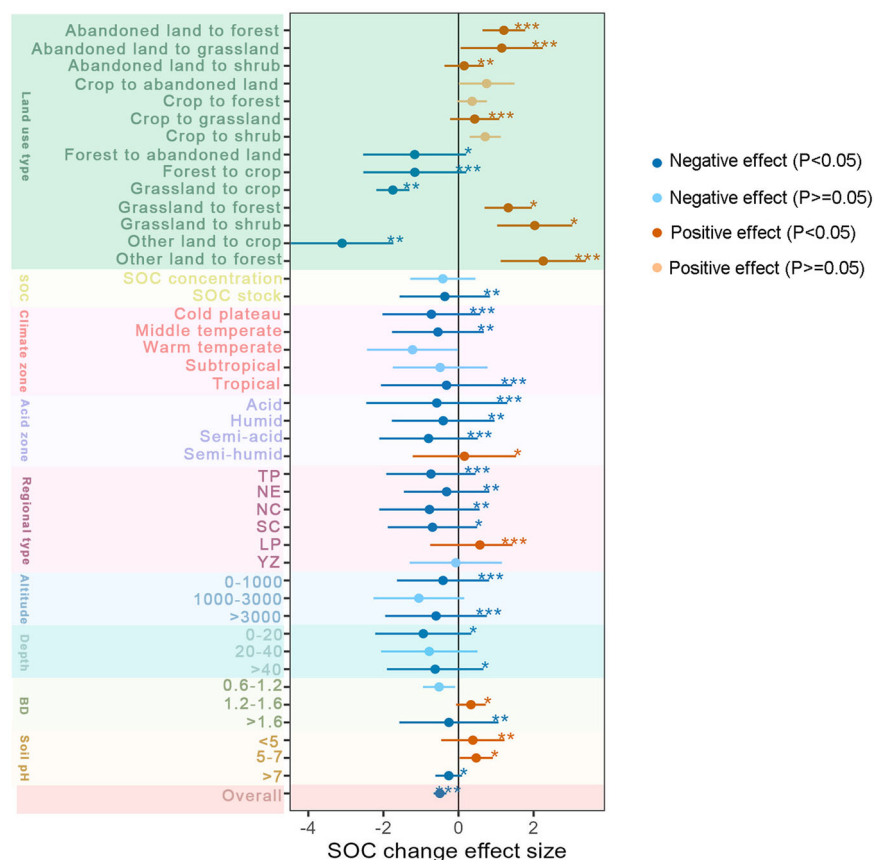
Historical Chinese land carbon cycle dynamic due to LUCC

To illustrate the impacts of LUCC on plant productivity, carbon sink dynamics, and carbon storage in China, we compared scenarios with and without LUCC from 1979 to 2014 using the CESM model. We validated the bias of carbon flux using FLUXNET data in China (Supplementary Fig. 4). The model captured well C dynamics in China using inventory-based forest C stock changes at both national and site levels as the validation dataset (Supplementary Table 6). The spatial distributions of mean annual GPP in simulations with and without LUCC gradually increased from northwest to southeast (Fig. 6a, b). Most western regions, characterized by land use types such as desert or plateau, exhibit GPP values lower than 500 g C m^{-2} yr^{-1}. Conversely, high GPP values (>1500 g C m^{-2} yr^{-1}) were frequently observed in southeast China, where both temperature and precipitation favor plant growth (Fig. 6a, b). Our findings showed the substantial impact of LUCC on the GPP trend, resulting in a cumulative increase of 6.65 PgC with a growth rate of 0.03 Pg C yr^{-1} from 1979 to 2014 (Fig. 6b). In contrast, under a scenario without LUCC during the same period, GPP was 7.01 PgC, indicating an annual decrease of 0.01 PgC (Fig. 6a). The observed trend of GPP due to LUCC (0.02 Pg C yr^{-1}) was nearly double that estimated by the no LUCC dataset (0.01 Pg C yr^{-1}). The LUCC-free scenario, which primarily considered climate, nitrogen deposition, and CO$_2$ fertilization, showed that LUCC has a more significant impact on altering land carbon uptake than climate (Fig. 6c). The CLM effectively captures well-known extreme climate events and natural disturbances, such as the 1986 drought, the 1991 eruption of Mount Pinatubo, and the strong El Niño of 1998 (Fig. 6c). The significant positive trends in GPP with LUCC, indicating enhanced carbon assimilation, were notable from 1979 to 2014 over a wide area (Fig. 7b). LUCC led to a rapid increase in carbon sinks within China's terrestrial ecosystems, particularly in the northwest, central China, and Qinghai-Tibetan Plateau regions following LUCC (Fig. 7b). Conversely, over the past four decades, the Central China region, along with the Yangtze River Delta and Pearl River Delta regions, has experienced a substantial reduction in GPP (Fig. 7a, b).

The LUCC-induced annual NEP in China was observed to be 2.53 g C m^{-2} yr^{-1} for the period from 1979 to 2014, contributing to a total terrestrial carbon uptake of 0.02 ± 0.12 Pg C yr^{-1} (Fig. 6e). Compared to the period without LUCC, the NEP was estimated at $-0.06 ± 0.16$ Pg C yr^{-1} (Fig. 6d). Carbon sink density exhibited an increase from northwest to southeast, with the largest carbon sink primarily distributed in southwest China (Fig. 6e). Additionally, mountainous regions such as Daxing'anling, Xiaoxing'anling, and the Changbai Mountains showed relatively high carbon sink values, exceeding 200 gC m^{-2} yr^{-1} (Fig. 6e). However, terrestrial ecosystems in most of Inner Mongolia, northwest China, and the hinterland of the Tibetan Plateau acted as carbon sources (Fig. 6d, e). Overall, our estimations suggest that approximately 80% of the area functions as a carbon sink in China (Fig. 6e). In terms of temporal trends, the LUCC-induced annual NEP demonstrated significant increasing patterns (Fig. 6f). Spatially, the notable trend of NEP predominantly manifested in high latitudes (Fig. 6d). LUCC positively influenced carbon sinks in China, leading to a significant enhancement in carbon sequestration compared to scenarios solely driven by climatic factors (NO LUCC). The average NEP trend value of 0.02 g C m^{-2} yr^{-1} indicated an upward trend in carbon sink capacity across most regions (Fig. 7d). Increased trends were primarily found in the Qinling Mountains and Loess Plateau, while declining trends were mainly concentrated in the southwest and northeast regions of China, especially in the southern Tibetan Plateau.

The spatial variations of land-induced carbon cycle

Soil carbon stock in topsoil (0–20 cm) was 73.33 ± 0.45 Pg C, while land-induced SOC stock in land-use-disturbed topsoil was 71.73 ± 0.56 Pg C (Supplementary Fig. 8). LUCC in the upper 0.2 m of soil resulted in a 1.6 Pg C carbon loss, indicating a significant decrease in SOC density due to anthropogenic LUCC 1979 to 2014. Our findings revealed that there was no statistically significant disparity in soil organic carbon (SOC) storage between the surface (0–20 cm) and deeper layers (20—100 cm) influenced by LUCC. The maximum SOC content in surface soil (0–20 cm) was
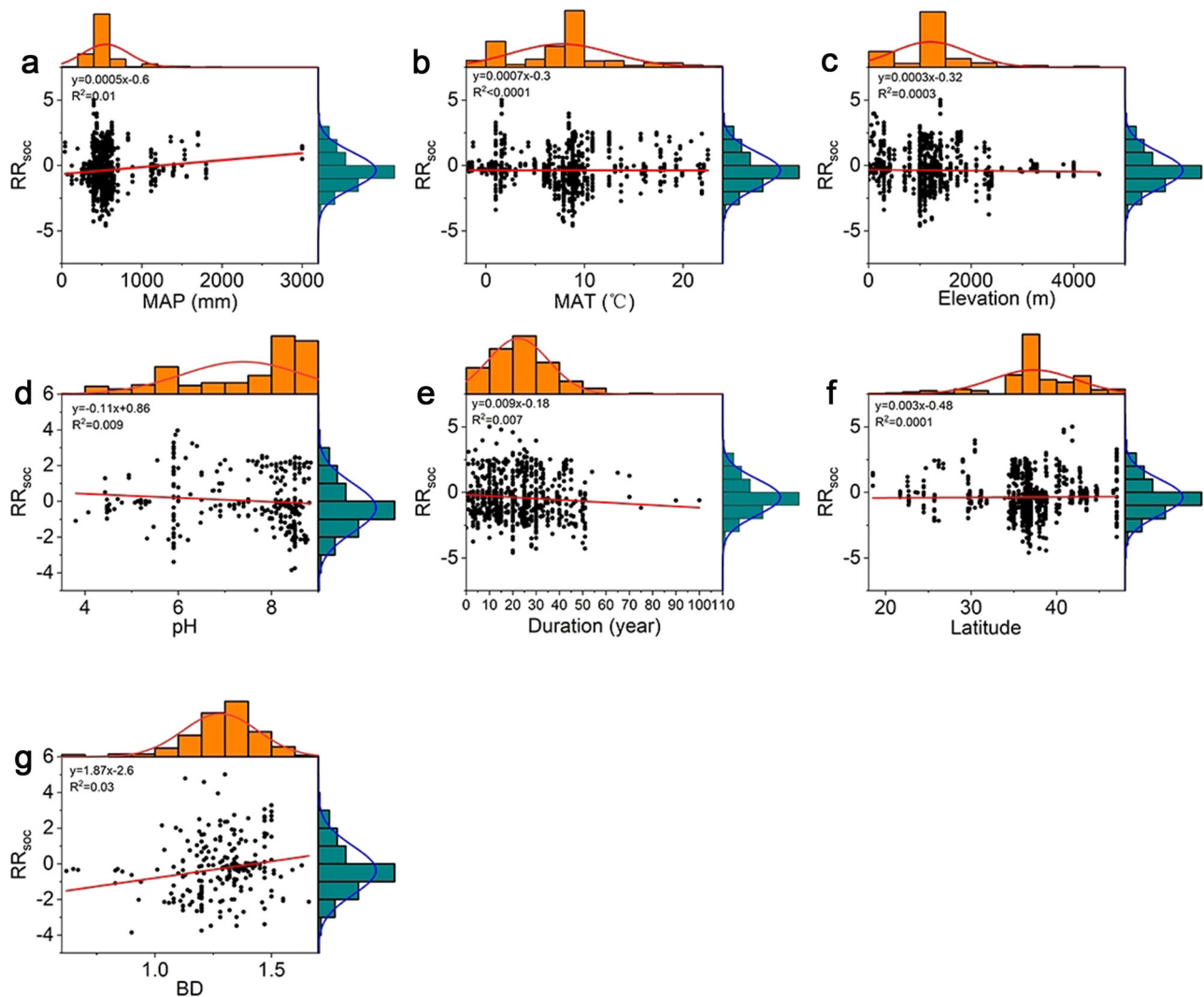
Fig. 4 | Meta-regression results (red line) showing relationships between soil (bulk density, pH), geographical elevation, latitude, mean annual temperature (MAT), mean annual precipitation (MAP), and land management factor (duration) and response ratios (RR) of SOC following LUCC in China. Individual data points show RR values for each observation. **a** MAP, **b** MAT, **c** elevation, **d** soil pH, **e** duration, **f** latitude, **g** bulk density.
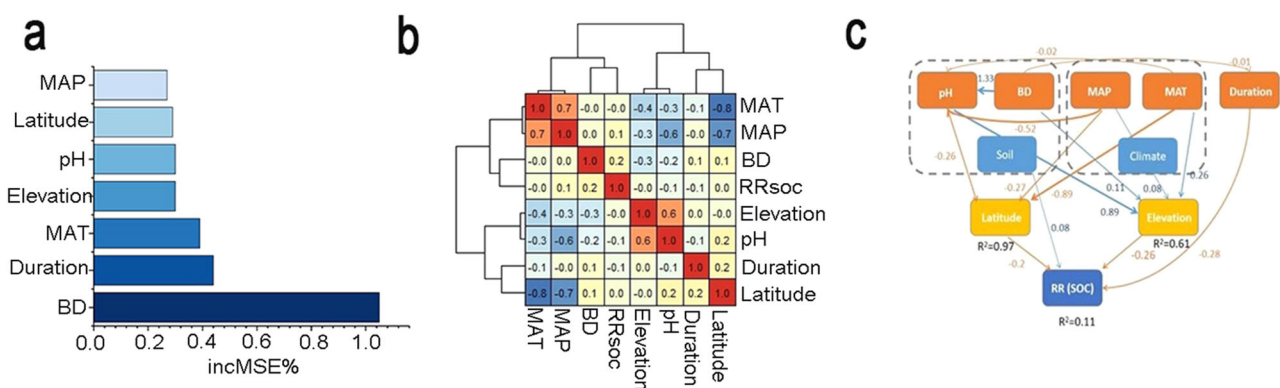

Fig. 5 | The abiotic and biotic drivers of SOC changes following LUCC. a The relative importance of environmental variables in influencing the response of SOC to LUCC. MAP, mean annual precipitation; MAT, mean annual temperature; BD, bulk density, (**b**) Correlations between climate, soil, duration, environmental factors, and SOC, (**c**) SEM for SOC, showing the relationships between climate, soil, duration, environmental factors and SOC. Significant paths are shown in blue if positive or in orange if negative. Numbers near the pathway arrow indicate the standard path coefficients. The portion of variance explained by the model (R^2) is shown for the response variable.
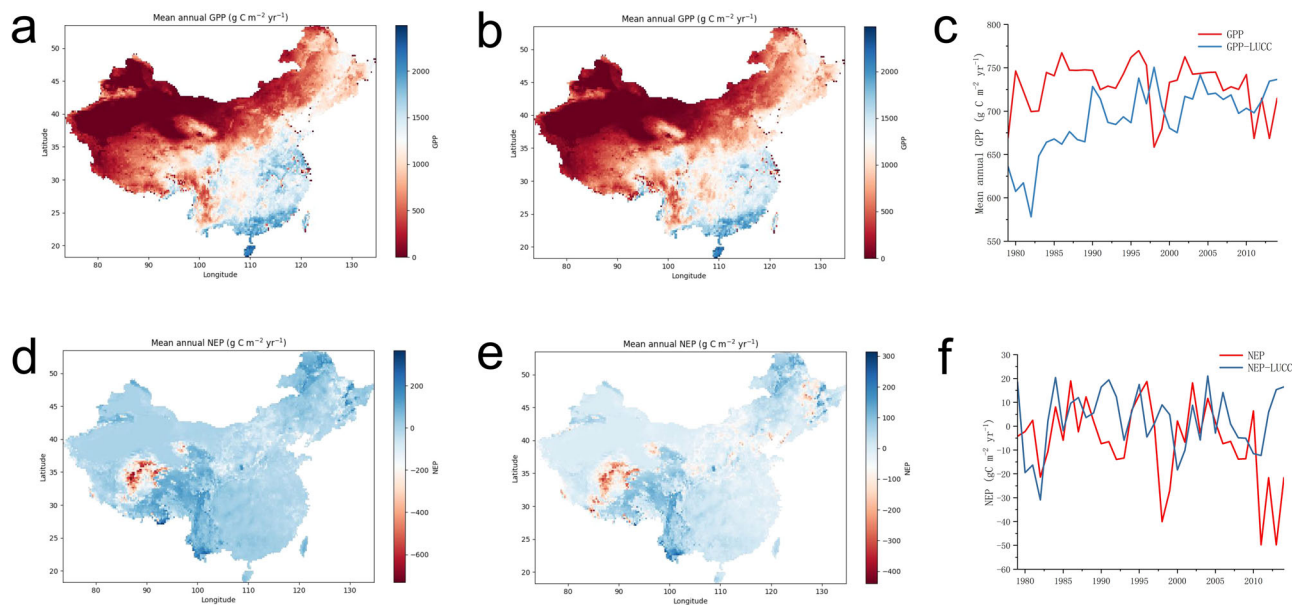
Fig. 6 | Land–atmosphere carbon fluxes over No LUCC and LUCC in China. The annual mean values for 1979–2014 were shown. **a** Spatial distributions of GPP over No LUCC, **b** Spatial distributions of GPP over LUCC, **c** The temporal variations of GPP over No LUCC and LUCC, **d** Spatial distributions of NEP over No LUCC, **e** Spatial distributions of NEP over LUCC, **f** The temporal variations of NEP over No LUCC and LUCC.
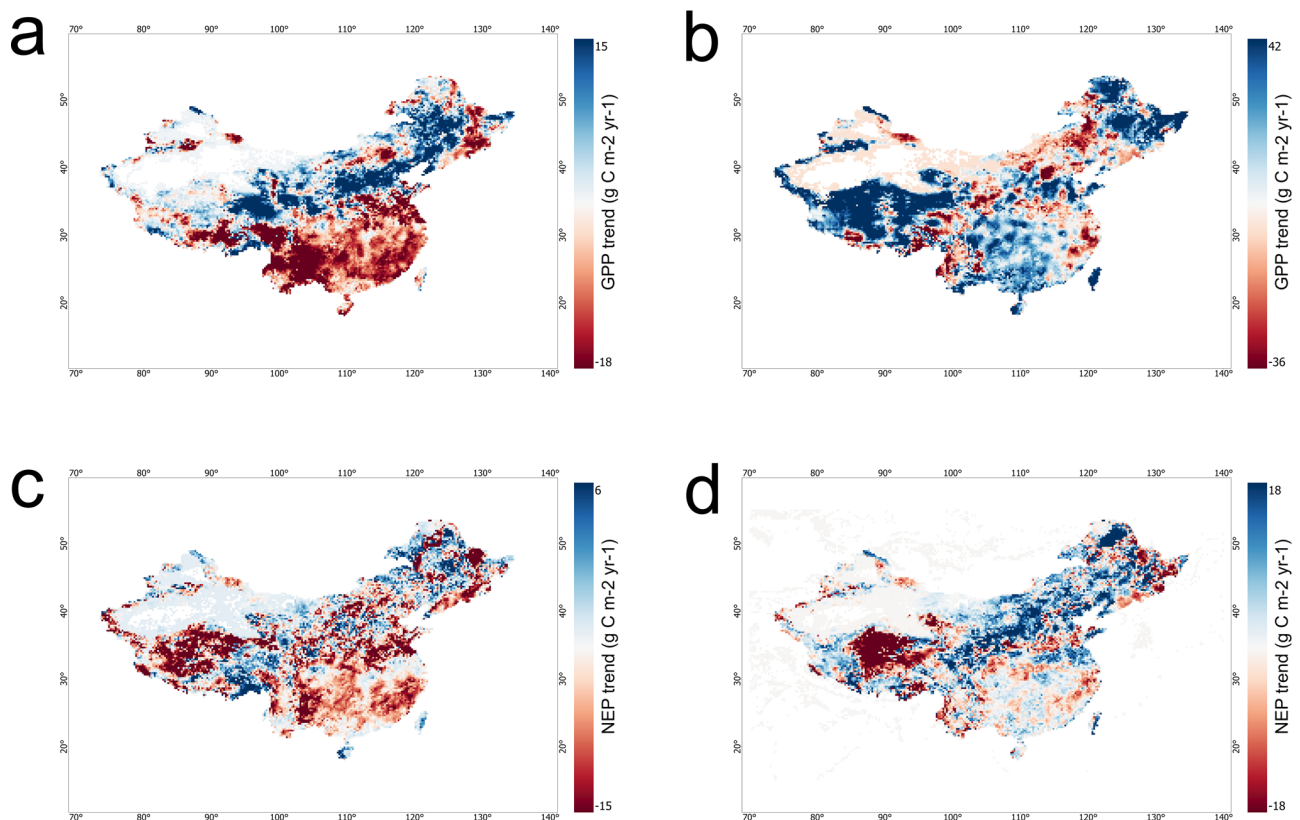

Fig. 7 | Trends of land carbon fluxes over No LUCC and LUCC in China. a Spatial distributions of GPP trends over No LUCC, **b** Spatial distributions of GPP trends over LUCC, **c** Spatial distributions of NEP trends over No LUCC, **d** Spatial distributions of NEP trends over LUCC.

300 kg C m^{-2}, while the average SOC in subsurface layer (20–40 cm) soil was 200 kg C m^{-2}. Soil carbon pools (0–100 cm) exhibit large spatial variations at the national scale (Supplementary Fig. 9c). Both No-LUCC and LUCC SOC density exhibited the highest soil carbon densities in regions such as the Xing'anling Mountains in Northeast China, the Qilian Mountains in Qinghai, the Tian Shan Mountains in northern Xinjiang, and the Tibetan Plateau (Supplementary Fig. 9a, b). However, the SOC density displayed complex variations: the land-induced SOC density has significantly decreased in regions observed in Jilin, Xinjiang, and Shanghai, with a minimum value of −1.69 kg C m^{-2} (Supplementary Fig. 9c). The

maximum differences in SOC density occurred in Tianjin, Jiangsu, and Henan provinces, with a maximum value of 3.65 kg C m^{-2} (Supplementary Fig. 9c). LUCC activities also decreased soil carbon pools (100 cm) significantly, with a minimum value of −1.06 kg C m^{-2}. However, LUCC in Tianjin, Jiangsu, Henan, and Shandong had a positive impact on surface SOC storage (Supplementary Fig. 9d, e, f).

China's land use practices significantly influence carbon fluxes within its ecosystems. Our analysis of carbon fluxes associated with litter and coarse woody debris (CWD) across China revealed a subtle spatial pattern (Supplementary Fig. 10). Generally, carbon fluxes were higher in southeastern China but lower in northwestern China, with most regions averaging 200 Tg C yr^{-1} (Supplementary Fig. 10a). However, the northeast region surpassed this average, with Shanghai and Jiangsu registering a peak flux of 96 Tg C yr^{-1} (Supplementary Fig. 10b). We observed a notable increase in wood product pools due to land cover change, particularly pronounced in Hainan, where it surged to 4.31 Pg C yr^{-1}. The cumulative addition to wood product pools due to land cover change unfolds as a substantial 40.16 Pg C yr^{-1} from 1979 to 2014 in China (Supplementary Table 7).

Understanding historical changes in land use and land cover further enriches our understanding of carbon dynamics in China. The results showed that the area of grasslands and forests changed from 1979 to 2014 (Supplementary Fig. 11). Specifically, while the overall area of grasslands increased, the area of C3 non-arctic grasslands increased by 66,100 m^2, and the area of C$_4$ grasslands increased, to 56,100 m^2 (Supplementary Table 8). In contrast, forest area in general shows complex dynamics. Different types of forests, including temperate evergreen conifers, arctic evergreen conifers, arctic deciduous conifers, tropical evergreen broadleaf, temperate evergreen broadleaf, tropical deciduous broadleaf, temperate deciduous broadleaf, arctic deciduous broadleaf, temperate deciduous broadleaf shrubs, and arctic deciduous broadleaf shrubs, have undergone changes in area of varying degrees. Overall, there has been a decrease in the total forest area, especially in the boreal region.

Discussion

Understanding the impact of LUCC on global elements, carbon cycles, and surface properties is crucial for addressing regional carbon balances. We report a previously overlooked role of LUCC in driving the land carbon cycle in China by using a three-level meta-analysis and taking the commonly used LUH2 to drive an ecosystem model. The meta-analysis serves a dual purpose: it validates the model results by providing empirical data, ensuring alignment between observed and simulated outcomes, while also minimizing uncertainties. By integrating meta-analytic data with modeling, we enhance the reliability of our findings without significantly impacting the conclusions drawn. This approach not only strengthens the robustness of our results but also underscores the importance of incorporating empirical data alongside modeling efforts to gain a comprehensive understanding of the complex interactions driving the land carbon cycle[38].

We found that LUCC caused a 39.2% loss of SOC change in China, with grassland conversion to cropland resulting (56%) in significantly higher losses than forest to cropland conversion (37%). This is consistent with previous studies[8,39,40], indicating that LUCC is a significant contributor to land carbon loss. Huang et al.[40] reported that forest-to-cropland conversion led to a global reduction in SOC of 24.5% ± 1.53%, while grassland-to-cropland conversion resulted in a reduction of 22.7% ± 1.22%. However, our study, which specifically focused on China, revealed a more precise loss percentage of 39.2% due to LUCC. This disparity highlights the heightened magnitude of SOC loss in China compared to the global averages[40]. This discrepancy can be attributed to several factors: previous studies primarily examined SOC stocks[41], whereas our study also considered SOC concentrations. Moreover, grasslands typically begin with higher initial SOC stocks compared to forests. For example, converting grassland to forest resulted in an 18% decrease in SOC stocks[42], suggesting that natural grasslands may maintain greater soil carbon stocks than natural forests.

Total soil profile carbon stocks are 13% higher in grasslands compared to forests[43], and grasslands possess significantly greater soil organic matter content[44]. Additionally, our approach utilized a three-level meta-analysis, providing a more comprehensive understanding of the impact of LUCC on SOC. Unlike traditional meta-analyses, our method allowed for the integration of multiple levels of data, thereby enhancing the accuracy and precision of our results.

Our study also found that LUCC has had a notably positive impact on SOC change in the Loess Plateau compared to other regions in China. This can be attributed to several factors. National policies, including the Three-North Shelterbelt Forest, Natural Forest Conservation Program, and GFGP, have significantly enhanced ecological conditions and brought about substantial LUCC changes[45]. Specifically, the GFGP has proven particularly effective in the Loess Plateau by converting farmland into grassland or forest and transforming barren land into productive areas[46,47]. Overall, the conversion of cropland to forest, grassland, and shrubland increased SOC by 11%, 13%, and 22%, highlighting the effectiveness of afforestation in climate change mitigation and biodiversity conservation[17,48,49].

LUCC-induced SOC losses were relatively minor in tropical climates compared to Temperate and Cold Plateau, indicating that climate plays a crucial role in shaping SOC dynamics[39,48,50]. Moreover, our results reveal that indirect climate effects, particularly soil bulk density, significantly impact SOC compared to direct climate effects, consistent with the previous study[36]. This can be explained by the fact that soil bulk density affects soil properties such as porosity, structure, and moisture retention, which in turn influence gas exchange and water movement, crucial for SOC decomposition and stabilization[51].

Based on LUH2 driving an ecosystem model, our study underscores the dominant role of LUCC in shaping the terrestrial carbon sink in China from 1979 to 2014. Our results reveal that the land-induced GPP trend of 0.02 Pg C yr^{-1} is twice as large as the GPP trend without land disturbance. However, certain regions (e.g., central China and Yangtze River Delta, Beijing-Tianjin wing) experienced a decline in GPP from 1979 to 2014, highlighting the spatial heterogeneity of carbon dynamics affected by rapid urbanization[17,48,52].

Our results also indicate that the NEP is sensitive to LUCC, resulting in enhanced carbon sink capacity within China's terrestrial ecosystems[17,22], especially in regions such as the northwest, central China, and Qinghai-Tibetan Plateau. Additionally, we found that carbon stocks in soils significantly decreased by 1.6 Pg C due to anthropogenic LUCC from 1979 to 2014 in China. It is important to note that China has implemented the Natural Forest Conservation Program (NFCP) and the Green Grain Program (GGP) to combat carbon loss from LUCC[53]. The NFCP focuses on banning logging in the southwest and reducing logging in other areas, while the GGP aims to increase grasslands and planted forests on sloping cropland and degraded grasslands[54]. However, since 1978, forest restoration policies have varied across China's provinces due to different management styles, resulting in inconsistencies in LUCC impact on the carbon cycle.

Our findings underscore the significant role of LUCC in shaping the historical carbon dynamics in China, emphasizing the imperative for afforestation and conservation practices to enhance carbon sequestration and mitigate the impacts of climate change. Our study also provides scientific guidance for future carbon management and climate change, highlighting the significant contribution of reforestation and afforestation in combating global climate change and enhancing carbon sinks. Through an ensemble of a three-level meta-analysis and state-of-the-art DGVMs, we have effectively depicted the long-term evolution of the land carbon cycle in China. Our results elucidate that LUCC has accelerated China's land carbon sinks, despite the limitation of soil carbon.

A comprehensive process-based understanding remains elusive due to several model and data limitations. Notably, the CESM and LUH2 datasets contain uncertainties in historical land-use data, initial input parameters, and physical processes. To address these limitations, we incorporated 1248 observed data points through a meta-analysis, employing a more

scientifically robust cross-scale approach. This methodological framework enhances the scientific rigor of our assessment, providing a more accurate understanding of how land-use changes have influenced China's terrestrial carbon cycle over historical periods.

For future research, it is crucial to prioritize efforts aimed at improving the accuracy of input parameters and refining the representation of physical processes within models. The uncertainty surrounding the above/below-ground partitioning of the carbon sink is attributable to the oversimplified representation of internal carbon cycling mechanisms[55]. To address this gap, enhancing models with improved plant allocation algorithms, refined tissue lifespan and mortality dynamics, and the incorporation of process-based soil carbon and nutrient cycling mechanisms should be prioritized in future research endeavors.

Data availability

Code availability

All computer codes for the analysis of the data are available from the corresponding author upon reasonable request.

References

1. Yue, C., Ciais, P., Houghton, R. A. & Nassikas, A. A. Contribution of land use to the interannual variability of the land carbon cycle. *Nat. Commun.* **11**, 3170 (2020).
2. Hurtt, G. C. et al. Harmonization of land-use scenarios for the period 1500–2100: 600 years of global gridded annual land-use transitions, wood harvest, and resulting secondary lands. *Clim. Change* **109**, 117 (2011).
3. Foley, J. A. et al. Global consequences of land use. *Science* **309**, 570–574 (2005).
4. Foley, J. A. et al. Solutions for a cultivated planet. *Nature* **478**, 337–342 (2011).
5. Stocker, T. F. et al. Contribution of working group I to the fifth assessment report of the intergovernmental panel on climate change. *Clim. Change* **5**, 1–1552 (2013).
6. Le Quéré, C. et al. Global carbon budget 2017. *Earth Syst. Sci. Data* **10**, 405–448 (2018).
7. Friedlingstein, P. et al. Global carbon budget 2020. *Earth Syst. Sci. Data Discuss.* **2020**, 1–3 (2020).
8. Houghton, R. A. et al. Carbon emissions from land use and land-cover change. *Biogeosciences* **9**, 5125–5142 (2012).
9. Ciais, P., et al. Carbon and other biogeochemical cycles. In Climate change 2013: the physical science basis. Contribution of Working Group I to the Fifth Assessment Report of the Intergovernmental Panel on Climate Change. 465–570 (Cambridge University Press, 2014).
10. Bangroo, S. A., Najar, G. R., Achin, E. & Truong, P. N. Application of predictor variables in spatial quantification of soil organic carbon and total nitrogen using regression kriging in the North Kashmir forest Himalayas. *Catena* **193**, 104632 (2020).
11. Villarino, S. H., Studdert, G. A., Laterra, P. & Cendoya, M. G. Agricultural impact on soil organic carbon content: testing the IPCC carbon accounting method for evaluations at county scale. *Agric. Ecosyst. Environ.* **185**, 118–132 (2014).
12. Lehmann, J. & Kleber, M. The contentious nature of soil organic matter. *Nature* **528**, 60–68 (2015).
13. Schmidt, M. W. et al. Persistence of soil organic matter as an ecosystem property. *Nature* **478**, 49–56 (2011).
14. Sanderman, J., Hengl, T. & Fiske, G. J. Soil carbon debt of 12,000 years of human land use. *Proc. Natl Acad. Sci.* **114**, 9575–9580 (2017).
15. Tian, J. et al. Microbially mediated mechanisms underlie soil carbon accrual by conservation agriculture under decade-long warming. *Nat. Commun.* **15**, 377 (2024).
16. Yang, F., He, F., Li, S., Li, M. & Wu, P. A new estimation of carbon emissions from land use and land cover change in China over the past 300 years. *Sci. Total Environ.* **863**, 160963 (2023).
17. Yu, Z. et al. Forest expansion dominates China's land carbon sink since 1980. *Nat. Commun.* **13**, 5374 (2022).
18. Yu, Z., Lu, C., Tian, H. & Canadell, J. G. Largely underestimated carbon emission from land use and land cover change in the conterminous United States. *Glob. Change Biol.* **25**, 3741–3752 (2019).
19. Peng, C. & Apps, M. J. Contribution of China to the global carbon cycle since the last glacial maximum: reconstruction from palaeovegetation maps and an empirical biosphere model. *Tellus B* **49**, 393–408 (1997).
20. Bonan, G. B. & Doney, S. C. Climate, ecosystems, and planetary futures: the challenge to predict life in Earth system models. *Science* **359**, eaam8328 (2018).
21. Fernández-Martínez, M. et al. Global trends in carbon sinks and their relationships with CO_2 and temperature. *Nat. Clim. Change* **9**, 73–79 (2019).
22. Deng, L. et al. Land-use changes driven by 'Grain for Green program reduced carbon loss induced by soil erosion on the Loess Plateau of China. *Glob. Planet. Change* **177**, 101–115 (2019).
23. Grassi, G. et al. The key role of forests in meeting climate targets requires science for credible mitigation. *Nat. Clim. Change* **7**, 220–226 (2017).
24. Lan, X. et al. Land-use intensity reversed the role of cropland in ecological restoration over the world's most severe soil erosion region. *Earth's Future* **11**, e2022EF003388 (2023).
25. Grassi, G. et al. Reconciling global-model estimates and country reporting of anthropogenic forest CO2 sinks. *Nat. Clim. Change* **8**, 914–920 (2018).
26. Burchett, M. D., Allen, C., Pulkownik, A. & MacFarlane, G. Rehabilitation of saline wetland, Olympics 2000 site, Sydney (Australia)—II: saltmarsh transplantation trials and application. *Mar. Pollut. Bull.* **37**, 526–534 (1999).
27. Gong, L. et al. Effects of vegetation restoration on soil organic carbon in China: a meta-analysis. *Chin. Geogr. Sci.* **27**, 188–200 (2017).
28. Brewer, M. J., Butler, A. & Cooksley, S. L. The relative performance of AIC, AICC and BIC in the presence of unobserved heterogeneity. *Methods Ecol. Evol.* **7**, 679–692 (2016).
29. Marín-Martínez, F. & Sánchez-Meca, J. Weighting by inverse variance or by sample size in random-effects meta-analysis. *Educ. Psychol. Meas.* **70**, 56–73 (2010).
30. Doi, S. A., Barendregt, J. J., Khan, S., Thalib, L. & Williams, G. M. Advances in the meta-analysis of heterogeneous clinical trials II: the quality effects model. *Contemp. Clin. Trials* **45**, 123–129 (2015).
31. Beillouin, D. et al. A global overview of studies about land management, land-use change, and climate change effects on soil organic carbon. *Glob. Change Biol.* **28**, 1690–1702 (2022).
32. Lajeunesse, M. J. On the meta-analysis of response ratios for studies with correlated and multi-group designs. *Ecology* **92**, 2049–2055 (2011).
33. Danabasoglu, G. et al. The community earth system model version 2 (CESM2). *J. Adv. Model. Earth Syst.* **12**, e2019MS001916 (2020).
34. Lawrence, D. M. et al. The community land model version 5: Description of new features, benchmarking, and impact of forcing uncertainty. *J. Adv. Model. Earth Syst.* **11**, 4245–4287 (2019).
35. Hurtt, G. C. et al. Harmonization of global land use change and management for the period 850–2100 (LUH2) for CMIP6. *Geosci. Model. Dev.* **13**, 5425–5464 (2020).
36. Jobbágy, E. G. & Jackson, R. B. The vertical distribution of soil organic carbon and its relation to climate and vegetation. *Ecol. Appl.* **10**, 423–436 (2000).
37. Post, W. M., Emanuel, W. R., Zinke, P. J. & Stangenberger, A. G. Soil carbon pools and world life zones. *Nature* **298**, 156–159 (1982).

38. Yuan, T. et al. Potential decoupling of CO_2 and Hg uptake process by global vegetation in the 21st century. *Nat. Commun.* **15**, 4490 (2024).
39. Lai, L. et al. Carbon emissions from land-use change and management in China between 1990 and 2010. *Sci. Adv.* **2**, e1601063 (2016).
40. Huang, X. et al. Land use change alters soil organic carbon: constrained global patterns and predictors. *Earth's Future* **12**, e2023EF004254 (2024).
41. Don, A., Schumacher, J. & Freibauer, A. Impact of tropical land-use change on soil organic carbon stocks—a meta-analysis. *Glob. Change Biol.* **17**, 1658–1670 (2011).
42. Jiao, Y., Xu, Z. & Zhao, Effects of grassland conversion to cropland and forest on soil organic carbon and dissolved organic carbon in the farming-pastoral ecotone of Inner Mongolia. *Acta Ecol. Sin.* **29**, 150–154 (2009).
43. Tate, K. R., Scott, N. A., Ross, D. J., Parshotam, A. & Claydon, J. J. Plant effects on soil carbon storage and turnover in a montane beech (Nothofagus) forest and adjacent tussock grassland in New Zealand. *Soil Res.* **38**, 685–697 (2000).
44. Stevenson, F. J. *Humus Chemistry Genesis, Composition, Reactions* (John Wiley & Sons, 1994).
45. Li, C., Zhang, Y., Shen, Y., Kong, D. & Zhou, X. LUCC-Driven changes in gross primary production and actual evapotranspiration in Northern China. *J. Geophys. Res. Atmos.* **125**, e2019JD031705 (2020).
46. Song, X., Peng, C., Zhou, G., Jiang, H. & Wang, W. Chinese Grain for Green Program led to highly increased soil organic carbon levels: a meta-analysis. *Sci. Rep.* **4**, 4460 (2014).
47. Tallis, H., Kareiva, P., Marvier, M. & Chang, A. An ecosystem services framework to support both practical conservation and economic development. *Proc. Natl. Acad. Sci.* **105**, 9457–9464 (2008).
48. Guo, L. B. & Gifford, R. M. Soil carbon stocks and land use change: a meta-analysis. *Glob. Change Biol.* **8**, 345–360 (2002).
49. Pan, Y. et al. A large and persistent carbon sink in the world's forests. *Science* **333**, 988–993 (2011).
50. Tang, X. et al. Carbon pools in China's terrestrial ecosystems: new estimates based on an intensive field survey. *Proc. Natl Acad. Sci.* **115**, 4021–4026 (2018).
51. Qiao, J., Zhu, Y., Jia, X., Huang, L. & Shao, M. Development of pedotransfer functions for predicting the bulk density in the critical zone on the Loess Plateau, China. *J. Soils Sediment.* **19**, 366–372 (2019).
52. Feng, H. et al. Contribution of land use and cover change (LUCC) to the global terrestrial carbon uptake. *Sci. Total Environ.* **901**, 165932 (2023).
53. Cheng, K. et al. Unveiling China's natural and planted forest spatial-temporal dynamics from 1990 to 2020. *ISPRS J. Photogramm. Remote Sens.* **209**, 37–50 (2024).
54. Dai, L. et al. Opportunities and challenges for the protection and ecological functions promotion of natural forests in China. *For. Ecol. Manag.* **410**, 187–192 (2018).
55. O'Sullivan, M. et al. Process-oriented analysis of dominant sources of uncertainty in the land carbon sink. *Nat. Commun.* **13**, 4781 (2022).

Author contributions
Y. Cheng and P. Luo conceived the project and designed the study. Y. Cheng performed the analyses and collected the data. M.W. Li and L.H. Wang assisted with data analysis. Y. Cheng and M.W. Li developed the model. Y. Cheng led the writing of the manuscript, with all co-authors (P. Luo, H. Yang, M.W. Li, M. Ni, H.L. Li, Y. Huang, W.W. Xie, and L.H. Wang) contributing with comments and inputs. All authors contributed critically to the drafts and gave final approval for publication.

Competing interests
The authors declare no competing interests.

Additional information
Supplementary information The online version contains supplementary material available at https://doi.org/10.1038/s41612-024-00751-w.

Correspondence and requests for materials should be addressed to Peng Luo.

Reprints and permissions information is available at http://www.nature.com/reprints

Publisher's note Springer Nature remains neutral with regard to jurisdictional claims in published maps and institutional affiliations.